Numerical simulation on tunnel spillway of Jingping-I hydropower project with four aerators

R Shilpakar[1,3], Z Hua[1], B Manandhar[1], N Shrestha[1], M R Zafar[1], T Iqbal[1] and Z Hussain[2]

[1]School of Renewable Energy, North China Electric Power University, Beijing 102206, China
[2]Pir Mehr Ali Shah-Arid Agriculture University, Rawalpindi, Pakistan

E-mail: razesh@ncepu.edu.cn

Abstract. This Study presents the results of a three dimensional simulation of a tunnel spillway with four aerators of Jingping-1 hydropower project as done by using ANSYS. The study uses a combination of realizable k-ε turbulence model and volume of fluid method in order to simulate the characteristics of aeration and cavitation in aerated tunnel spillway. It is possible to yield the water surface profile, pressure distribution, velocity profile and aeration cavity length from the simulation. Results of numerical simulation were compared with experimental results showing that the realizable k-ε turbulence model and volume of fluid model can simulate the aerated tunnel spillway. The aerated cavity zone was found to be stable and within reasonable length. Results from the numerical simulation were found to resemble the experimental result to a great extent, showing the validity of the simulation.

1. Introduction

There is more of cavitation in high velocity and high pressure head in free-flow tunnel spillway. Artificial aerators are generally introduced to reduce cavitation which is very cost-effective and easy measures. Different researches have been done in the study of aeration phenomenon. Chanson [1] has explained the mechanism of aeration by showing that a large amount of air is introduced in the aeration zone along with the air water interface of jet and strong de-aeration tends to occur when undergoing the bottom near nappe impact. In spite of the strong de-aeration occurring in the impact point region, the bottom aerators are found to be very useful for introducing large amount of air over short distance. Pfisher [2] has conducted a hydraulic model test using typical chute aerators with various kinds of flow features including pre-aeration. The study has shown that the pre-aeration in the downstream of the aerators affect the stream-wise development and the bottom air concentration. Chanson [3] has established the method for calculating the cavity length in the bottom and side of sudden enlargement and vertical drop aerator. Both experimental and simulation methods were used to study the aeration in the spillways. Shuai Li et al [4] have presented a study on the diffused downstream flow from a radial sluice and full section aerator where a realizable k-ε turbulent model was combined with a mixture multiphase model. Shuai Li et al [5] have studied the aeration effect of the bottom as well as the side wall of a connective tunnel with high head and large discharge using an experimental test with numerical simulation. Results showed a reduced amount of back water effect in the aeration cavity with the increasing aeration length. Caihuan et al [6] proposed the optimization methods for radial gate with sudden enlargement and offset aerator, Jinhua et al [7] have concluded

that the air concentration is affected by the air-cavity length; Piller et al [8] have successfully simulated the turbulent flow in a channel and has obtained the improvement in the results, concluding on the influence of Prandtl number Pr on turbulent transport. Deng et al [9] have revealed the possibility of simulating the complicated flow in the tunnel spillway through the combining k-ε double equations turbulence model and volume of fluid method. Wu J H et al [10] have focused on the necessary of special designs on the different configuration and sizes of the aerators in various tunnel spillways where flow velocity is exceeding 40 m/s. In this study, the realizable k-ε turbulence model was used in a combination with the VOF method in order to determine the characteristics of aerated tunnel spillway in Jingpin-1 Hydropower Station. Jingping-I hydropower project is a tall arch dam located at the Jingping bend of Yalong river, Liangshan, Sichuan province, China. The capacity of this project is 3600 MW and has the tallest 305 m high arch dam. The total length of the flood tunnel spillway is 829 m where the length of the power tunnel is 434 m. The tunnel is free-aerated as air is also provided to the top of tunnel through ventilation shaft. Four aerators are inserted at four different sections. The aerators used here is the combination of deflector and offset type. The designed discharge of the project is 3229 m^3/s and the normal flow at 1880m [11]. The details of the projects were shown in the figure 1.

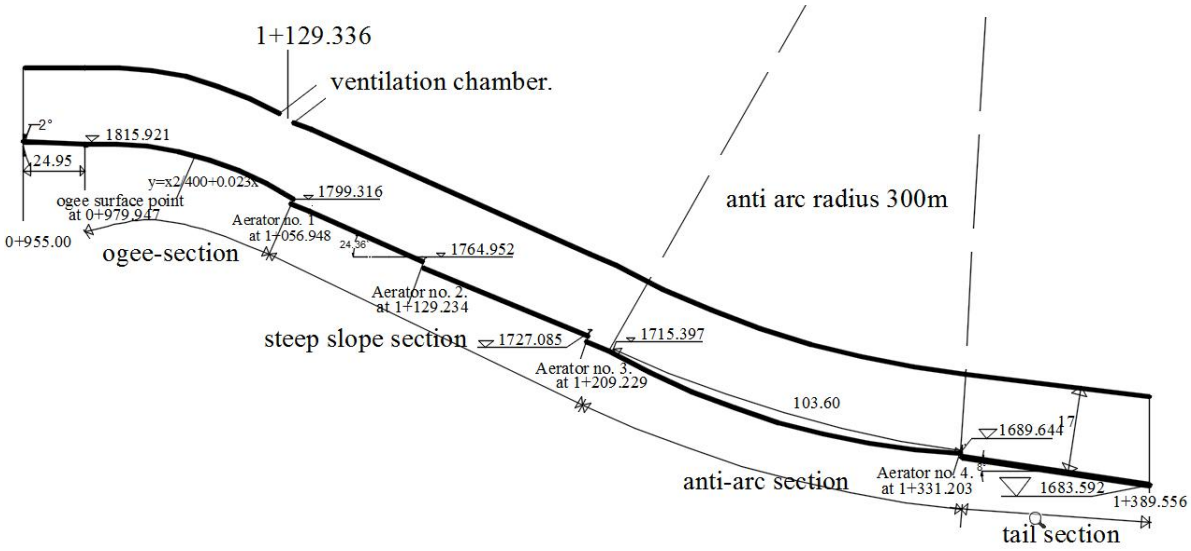

Figure 1. Detailed section of the free-aerated flood tunnel spillway [11].

2. Mathematical model

The realizable k-ε turbulence model has been used to solve the air-water flow .The instantaneous continuity, momentum and energy equations are expressed for a compressible liquid in the following manner.

Continuity equation:

$$\frac{\partial \rho}{\partial t} + \frac{\partial}{\partial x_i}(\rho u_i) = 0 \tag{1}$$

Momentum equation:

$$\frac{\partial}{\partial t}(\rho u_i) + \frac{\partial}{\partial x_j}(\rho u_i u_j + p\delta_{ij} - \tau_{ij}) = 0 \tag{2}$$

Energy equation:

$$\frac{\partial}{\partial t}(\rho \varepsilon_0) + \frac{\partial}{\partial x_j}\left(\rho u_j \varepsilon_0 + u_j p + q_j - u_i \tau_{ij}\right) = 0 \tag{3}$$

From stokes law, the viscous stress for a Newtonian fluid is

$$\tau_{ij} = 2\mu S_{ij}^{*} \tag{4}$$

Where trace less viscous strain rate is given by:

$$S_{ij}^{*} = \frac{1}{2}\left[\frac{\partial u_i}{\partial x_j} + \frac{\partial u_j}{\partial x_i}\right] - \frac{1}{3}\frac{\partial u_k}{\partial x_k}\delta_{ij} \tag{5}$$

Where u represents velocity, p represents pressure, ρ represents density and μ represents viscosity.

Turbulent flows are characterized by rapid fluctuations of velocity, density, temperature and concentration. The cause for such temporal fluctuations is the non-linear character of the physical-chemical processes. Turbulence is related with random fluctuations of fluid. The most of the engineering flows are turbulent. The transient velocity (being expressed as an instantaneous velocity), which is very difficult to predict due to its random occurrence with time. Instead, velocity is expressed into its steady mean value $\overline{u}_i$ with a fluctuating component $u_i^{'}$ in the following form:

$$u_i = \overline{u}_{i+} u_i^{'}$$

This process of time averaging is called Reynolds decomposing. This decomposition integrates the instantaneous continuity and momentum equation yielding the Reyonlds Averaged Navier-Strokes (RANS) equations:

$$\frac{\partial}{\partial t}(\rho u_i) + \frac{\partial}{\partial x_j}\left(\rho u_i u_j\right) = -\frac{\partial p}{\partial x_j} + \left[\mu\left(\frac{\partial u_i}{\partial x_j} + \frac{\partial u_j}{\partial x_i} - \frac{2}{3}\delta_{ij}\ \frac{\partial u_k}{\partial x_k}\right)\right] + \frac{\partial}{\partial x_i}\left(-\rho\overline{u_i^{'}u_j^{'}}\right) \tag{6}$$

There are many closure model exits but this paper presents only two-equation turbulence models. The Boussinesq hypothesis postulated that effect of turbulence can be represented as an increased viscosity, it is called viscosity model.

$$\left(-\rho\overline{u_i^{'}u_j^{'}}\right) = \mu_t\left(\frac{\partial u_i}{\partial x_j} + \frac{\partial u_j}{\partial x_i} - \frac{2}{3}\delta_{ij}\ \frac{\partial u_k}{\partial x_k}\right) - \frac{2}{3}\rho k\delta_{ij} \tag{7}$$

RNG k-ε turbulence model and the realizable k-ε turbulence models are two improvement forms of the classical k-ε turbulence model applied in fluent. The realizable k-ε turbulence model guarantees the satisfactory results for rotational flows, flows with adverse gradients within their boundary layers and flows with separation-recirculation effects. In realizable k-ε turbulence model, the transport equation for k and ε are given as:

- For turbulent Kinetic energy (k)

$$\frac{\partial(\rho k)}{\partial t} + \frac{\partial}{\partial x_i}(\rho k u_i) = \frac{\partial}{\partial x_j}\left[\left(\mu + \frac{\mu_t}{\sigma_k}\right)\frac{\partial k}{\partial x_k}\right] + P_k + P_b - \rho_e - Y_m + s_k \tag{8}$$

- For dissipation (ε)

$$\frac{\partial(\rho\varepsilon)}{\partial t} + \frac{\partial}{\partial x_j}(\rho\varepsilon u_j) = \frac{\partial}{\partial x_j}\left[\left(\mu + \frac{\mu_t}{\sigma_\varepsilon}\right)\frac{\partial\varepsilon}{\partial x_j}\right] + \rho C_1 s_\varepsilon - \rho C_2 \frac{\varepsilon^2}{k+\sqrt{v\varepsilon}} + C_{1\varepsilon}s_\varepsilon\frac{\varepsilon}{k}\ C_{3\varepsilon}\rho_b\ s_\varepsilon \tag{9}$$

Where

$$C_1 = max\left[0.43, \frac{\eta}{\eta+5}\right],\quad \eta = S\frac{k}{\varepsilon}\ ,\quad S = \sqrt{2s_{ij}}s_{ij}$$

μ_t Represents turbulent viscosity calculated by the turbulent kinetic energy (k) and turbulent dissipation rate (ε) as:

$$\mu_t = \rho C_\mu \frac{k^2}{\varepsilon} \tag{10}$$

Where C_μ is no longer a constant which depends on the rate of rotation and strain rate, it is expressed as

$$C_\mu = \frac{1}{A_0 + A_s U^* k/\varepsilon} \tag{11}$$

A_0=4.0, $A_S=\sqrt{6}\cos\left\{\frac{1}{3}\cos^{-1}\left[\sqrt{6}\left(\frac{s_{ij}s_{jk}s_{ki}}{\sqrt{s_{ij}s_{ij}}}\right)\right]\right\}$, $U^* = \sqrt{s_{ij}s_{ij} + (\Omega_{ij} - 2\varepsilon_{ij}\,\omega_k)(\Omega_{ij} - 2\varepsilon_{ij}\,\omega_k)}$

The time average rotation rate tensor, $\Omega_{ij} = \frac{1}{2}\left[\frac{\partial u_i}{\partial x_j} + \frac{\partial u_j}{\partial x_i}\right]$.

VOF method is used to track and locate the free contact surfaces between phases. In this study, VOF method was applied for water phase and air phase. The sum of all the volume fractions is equal to one in each control volume. In this research, air is assumed as the first phase and water is assumed as the second phase. For air, the transport equation has the form as:

$$\frac{\partial(\alpha_a)}{\partial t} + \nabla.(\vec{V}\alpha_a) = 0 \qquad (12)$$

For the volume fraction α_a of the kth fluid, three conditions are possible; $\alpha_a = 0$ showing; the cell is empty in kth fluid, $\alpha_a = 1$ showing; the cell is full in kth fluid and $0 < \alpha_a < 1$ showing; the cell contain an interface between the fluids.

3. Computational domain and mesh

The flow over the tunnel spillway was modelled in 3-Dimensions in Computational fluid Dynamics (CFD). The geometry of the spillway with different types of aerators was drawn in ANSYS. The meshing of the geometry was done on GAMBIT software. The structural grid meshing was done from the geometry. The grid was made of hexahedral-cells (hex-mesh) on the whole domain. A finer mesh size was considered for better result. The mesh size of 0.4 m was set for hexahedral meshing. It resulted in a mesh volume of 780,000 cells with skewness 0.5. The meshing of the power tunnel was shown in figure 2.

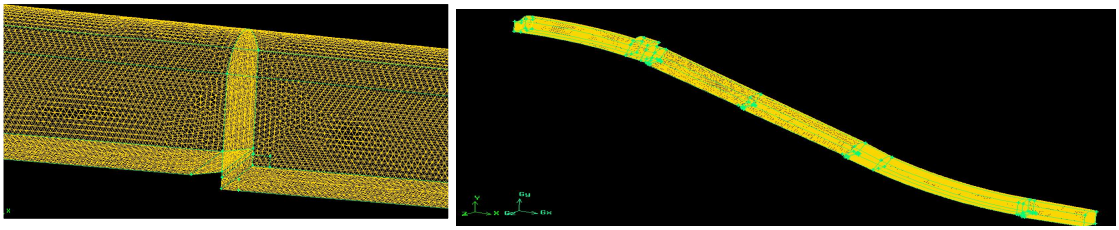

Figure 2. Meshing of the power tunnel.

4. Boundary condition and calculation

Pressure inlet was applied as a boundary condition to the inlet of the water domain where the static pressure developed due to the upstream water level of reservoir of 1880 m. Standard wall functions were used in the bottom surface and the side walls. Pressure boundary was applied on the area above water surface with atmospheric condition for the open channel flow and the outlet boundary was set to a pressure-outlet type with atmosphere. The pressure-based segregated solver was used in ANSYS and the default algorithm. The PISO pressure-velocity coupling scheme was used for the transient flow calculation. PISO can maintain the relatively stable condition when using a large time-step or mesh with a high degree of distortion. An implicit scheme was used with VOF method with default volume fraction cut-off. Realizable k-ε turbulence model with standard wall functions was employed. The Least Square Cell-based method was chosen for interpolation methods. Presto scheme was used as interpolation methods for pressure. The solution was initialized with the standard initialization methods and computed from water-inlet. The patching was done in the assumption that air was initially inside the tunnel before releasing water. The 0.02 time-step size was chosen and the simulation was done for 6000 numbers of time steps for about 120 seconds.

5. Results and discussion

Following are the results obtained from the simulation of the power spillway with four aerators.

5.1. Water surface profile and pressure distribution

Water surface profiles of the power tunnel obtained from the simulation and experimental results [11] for full flow is shown in figure 3. Water surface profile near in all four aerators have small risen due to deflector of aerator. Due to aeration from the upper ventilation pipe and bottom aerators, the water surface at the tail region of tunnel has been more aerated and in milky appearance. The calculated water surface is nearly close to the experimental results [11]. The development of negative pressure inside the tunnel of high velocity region causes cavitation. So, the bottom pressure distribution is important for better understanding. The figure 4 shows the comparison of bottom pressure distributions between simulation and experimental value inside the full flow tunnel spillway.

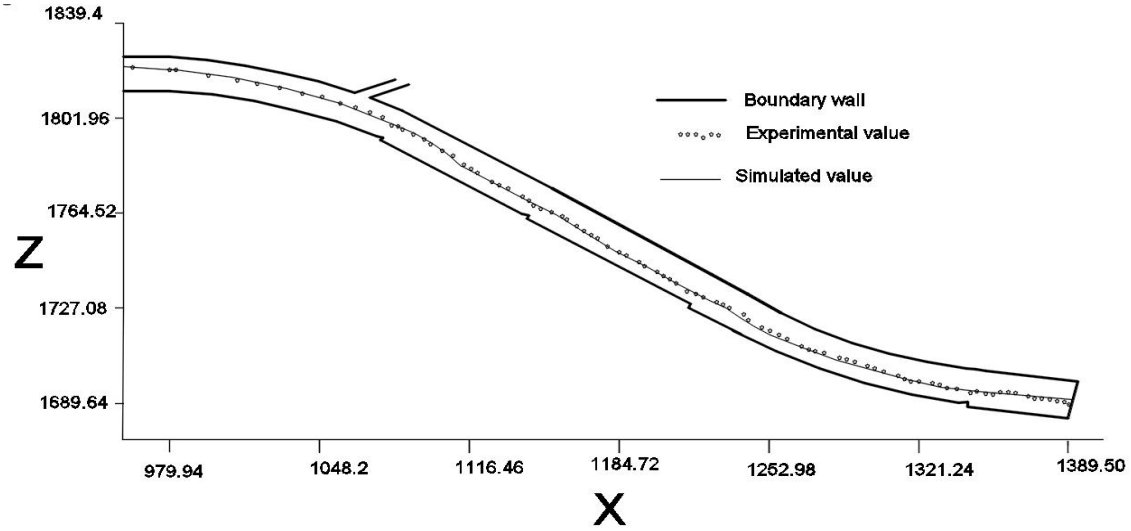

Figure 3. Comparison of water surfaces.

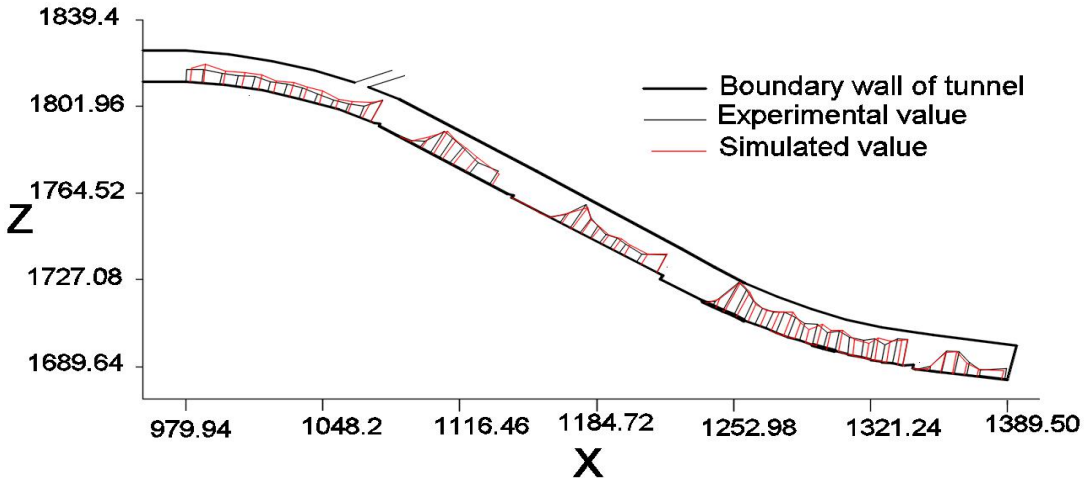

Figure 4. Comparison of bottom pressures inside the tunnel.

The simulated bottom plate pressures distribution on the tunnel spillway is nearly close with that of experimental values [11]. The table 1 clearly shows the bottom pressure developed inside the tunnel for full flow. The simulated bottom plate pressures before aerators 1 & 2 are 120 kPa and 70 kPa which are slightly less than experimental values [11] by 2.75% and 9.88% respectively. The simulated bottom pressure before aerators 3 & 4 are 110 kPa and 135 kPa that are slightly greater than that of experimental values [11] by 7.63% and 0.37% respectively.

Table 1. Bottom pressure development before aerators.

Position	Experimental values [11]	Simulated values	
	Bottom plate pressure (kPa)	Bottom plate pressure (kPa)	Error (%)
Before aeration #1	123.4	120	2.75
Before aeration #2	77.68	70	9.88
Before aeration #3	102.2	110	-7.63
Before aeration #4	134.5	135	-0.37

The figure 5 clearly shows the maximum bottom pressure developed at the floor of the tunnel for fully open gate after each aerator. The aerator jets influenced the pressure distribution in the floor of the spillway where low pressures are obtained near aerators and gradually increases its value to peak value. In the figure 5, blue color shows the low pressure region and red color shows peak value. The calculated peak pressures values in the bottom of spillway after the aerators #1, #2, #3 and #4 are 148 kPa, 135 kPa, 171 kKa and 115 kPa respectively. In aerated cavity, low pressures are obtained which ensured the effective aeration and the minimum pressure of 1.8 kPa,-5.75 kPa,-1.12 kPa and -7 kPa are observed after aerator position's #1, #2, #3 and #4 respectively. The maximum bottom pressure distribution after aerator #2 and # 4 are slightly less than that of experimental results [11]. The peak bottom pressure distribution after aerators #1 and #3 have slightly higher value than that of experimental results [11].

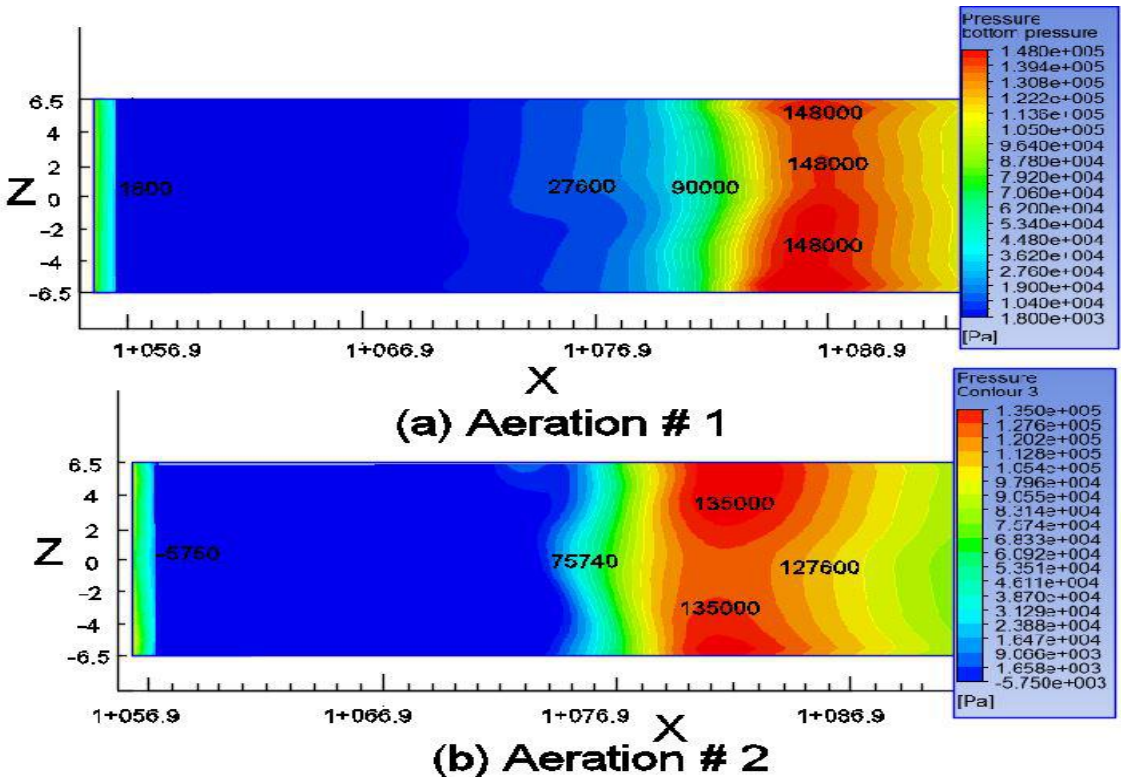

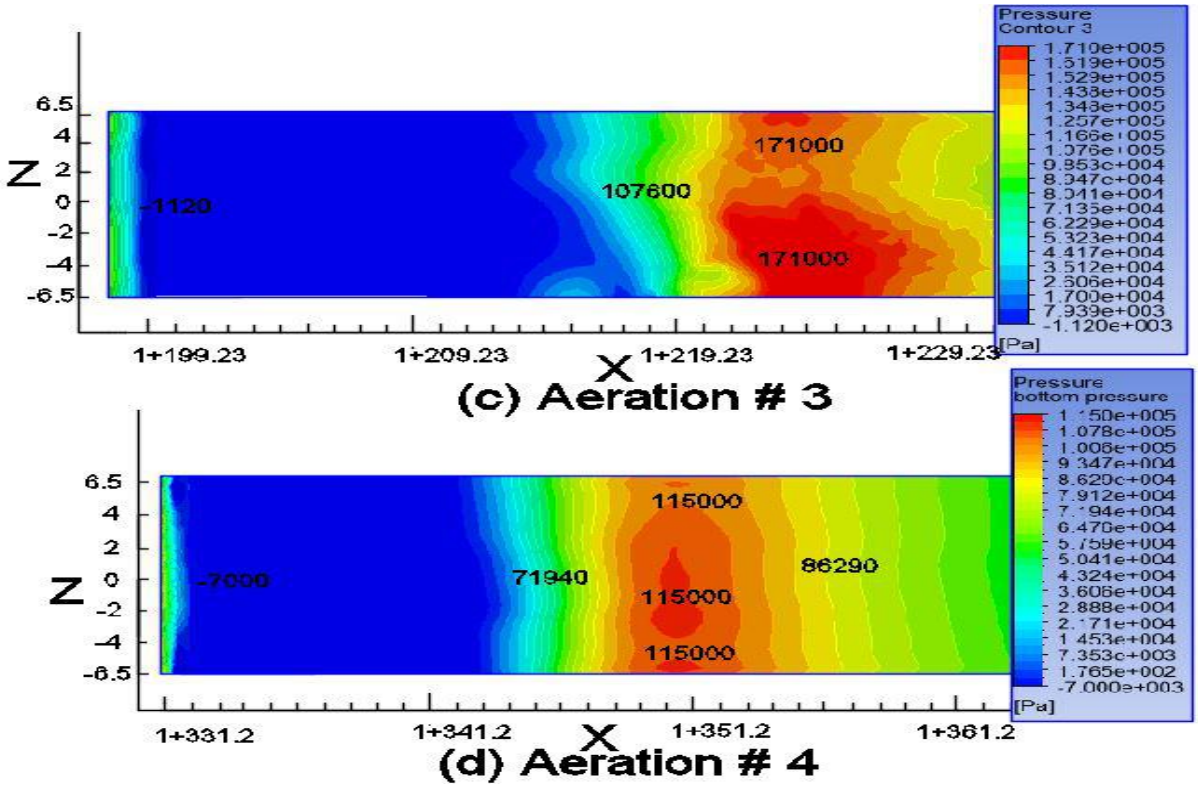

Figure 5. Maximum bottom pressure distributions.

5.2. Velocity distribution

Velocity is one of the most important hydraulic characteristics of the flow. Velocity determines the magnitude of the cavitation erosion. The velocity distribution of the full flow inside tunnel spillway with normal discharge at 1880 m before aerator #1 in the ogee section in the cross section is somehow linear because of no bottom aeration prior aerator #1. The velocity distribution of this ogee section is similar with that of the open channel flow. But the flow before aerator #2 is different from previous, where velocity contour is raised in the middle of the bottom boundary and distributed symmetrically on both sides due to aeration from aerator #1. Similarly, the velocity contour before aerator #3 at the middle of bottom is raised at that time of flow. The velocity distribution is changed due to aeration from the aerator. Water in the tail section of the free-aerated tunnel has been much more aerated and milky in appearance. Following figure 6 gives a detail of velocity development in the cross section of the free-aerated tunnel before aerator.

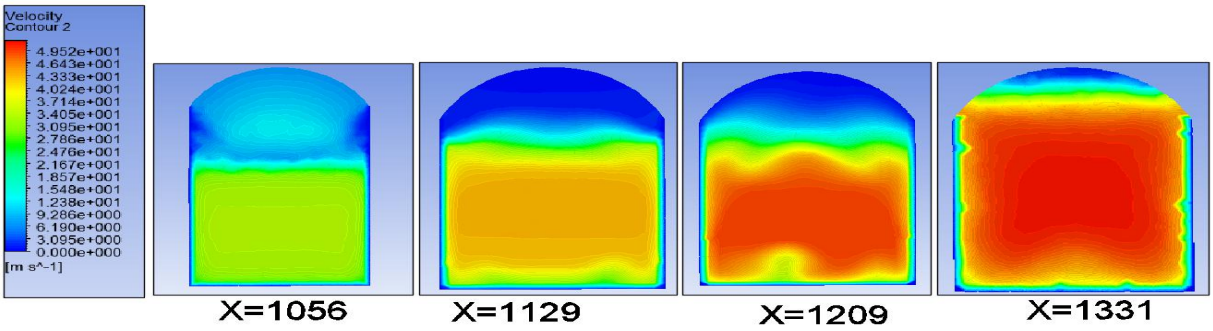

Figure 6. Flow Velocity in the cross section before aerator.

The average velocity and cavitation number of the fully flow in the cross section of the free-aerated tunnel before the aerators is shown in the table 2. The velocity of the flow near aerator #1 is 27.9 m/s, which is less than experimental value [11] with the relative error of 3.46%. The average velocity along the downstream of the tunnel gradually increased up to the end of the tunnel. The average velocity of the flow at the tail section of the tunnel before aerator #4 is obtained to be 46.4 m/s with the relative error of 5.46 % than that of the experimental result [11]. The maximum relative error does not exceed more than 6% which shows that the simulation result agrees well with the experimental result [11]. The cavitation numbers determine the cavitation damages. Aerators are kept in spillway to keep the cavitation index higher than 0.20. The minimum cavitation number obtained from simulation is 0.21 which shows that tunnel surface is free from cavitation damages.

Table 2. Average velocity and cavitation number.

Aerator's Position	Before Stake number	Average velocity (m/s)				
		Experimental Value [11]	Cavitation Number	Simulated value	Error%	Cavitation Number
Aerator # 1	1+056.94	28.9	0.49	27.9	-3.46	0.54
Aerator #2	1+129.23	35.8	0.25	35.7	-0.28	0.26
Aerator #3	1+209.22	41.9	0.21	42.09	0.45	0.23
Aerator # 4	1+331.20	44.0	0.22	46.40	5.45	0.21

5.3. Aeration features

In order to ensure full aeration, there shouldn't be backwater effect after the jump and should possess the stable shape and certain length of aerated cavity. The aeration cavities for fully opening gate inside the power tunnel spillway of four aerators are shown in figure 7. The red and blue color shows water and air respectively in the figure. Low Froude number is obtained near aerator #1 and stable aeration cavity is difficult to form. The impact angle of the jet tip on the slope obtained to be low which has helped in the reducing backwater effect and obtaining stable aeration cavity. The stable aeration cavities are formed after aerator #2, #3 and #4.

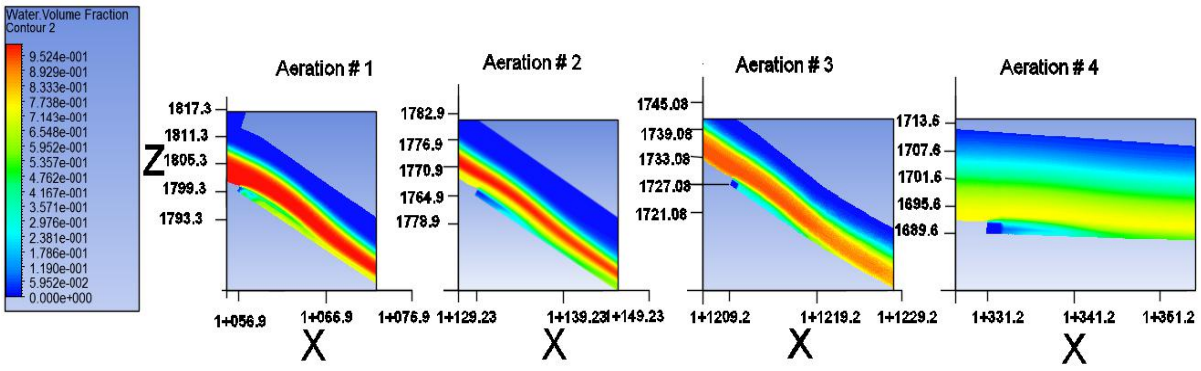

Figure 7. Bottom cavity of four aerators.

The comparative study of aeration cavity for full flow in the power tunnel between the numerical simulation and experimental results is shown in table 3. From the table, it can be easily figured out that the simulated aeration cavity length of 1# aerator is greater than experimental value [11] by 9.8%. But, the aeration cavity length of 2 # aerator is slightly smaller than that of experimental value [11] by 3.8%. The simulated aeration cavity length of 3 # aerator is larger than the experimental results [11] whereas simulated aeration cavity length of 4# aerator is smaller than the experimental results [11]. In aggregate, the simulated results agree with the experimental results [11].

Table 3. The Comparison of aerated cavity length.

Aerator	Aerated cavity length (m)		
	Simulated Value	Experimental Value [11]	Error (%)
1	28	25.5	9.8
2	26	27	-3.8
3	25	24	4.1
4	21.5	22.4	-4

6. Conclusion

The combination of Realizable k-ε turbulence model and VOF method were successfully used to simulate the flow characteristics in aerated tunnel spillway of Jingping-1 Hydropower Project. Other achievements could be presented in following points:

- The numerical simulation results were very similar to that of the experimental results.
- The bottom pressure distribution was reasonably distributed with that of the model test result as the maximum relative error of the pressure is less than 10%.
- Due to the insertion of aerators, there was variation in the velocity of flow. The air entrainment from the both sides of the wall has helped in the symmetrical distribution of the high velocity zones in the cross-section. The relative error of the average velocity didn't exceed 6% which agreed with the result from model test.
- The aerated cavity zone was stable and in reasonable length. The minimum cavitation number (0.21) among calculated was obtained at tail end of tunnel which was greater than 0.2 and justified the necessity of aerators.

Acknowledgments

This paper was a part of master thesis in the field of water resource and hydropower engineering. Authors are indebted to Mr. Sun Shuang Ke of China Institute of Water Resource and Hydropower Research for providing the necessary data.

References

[1] Chanson H 1994 Aeration and de-aeration at bottom aeration devices on spillways *Can. J. Civil. Eng.* **21(3)** 404-9
[2] Pfister M, Lucas J and Hager W H 2011 Chute aerators: Pre-aerated approach flow *J. Hydraul. Eng.* **137(11)** 1452-61
[3] Chanson H 1989 Study of air entrainment and aeration devices *J. Hydraul. Res.* **27(3)** 301-19
[4] Li S, Zhang J, Xu W, Chen J and Peng Y 2016 Evolution of pressure and cavitation on side walls affected by lateral divergence angle and opening of radial gate *J. Hydraul. Eng.* **142(7)** 05016003
[5] Li S, Zhang J, Xu W, Chen J, Peng Y, Li J and He X 2016 Simulation and experiments of aerated flow in curve-connective tunnel with high head and large discharge *Int. J. Civ. Eng.***14(1)** 23-33
[6] Caihuan Wang, Dongmei Hou, Li Li and Xia Yu 2012 Study of shape design of the aerator with sudden lateral enlargement and bottom drop behind high-head radial gate and its engineering application *J. Hydroelectr. Eng.* **31(5)** 107-13 (in Chinese)
[7] Wu J-H and Ruan S P 2007 Emergence angle of flow over an aerator *J Hydrodynam B* **19.5** 601-6
[8] Piller M, Enrico N and Thomas J H 2002 DNS study of turbulent transport at low Prandtl numbers in a channel flow *J. Fluid Mech.* **458** 419-441
[9] Deng J, Xu W L, Lei J and Diao M J 2005 Numerical simulation of hydraulic characteristics of high spillway tunnel *J. Hydroelectr. Eng*. **36(10)** 1209-18 (in Chinese)
[10] Ruan S P, Wu J H, Wu W W and Xi R Z 2007 Hydraulic research of aerators on tunnel

spillways *J Hydrodynam B* **19.3** 330-4
[11] China Water Conversancy and Research Institute 2011 The Model Test of the Flood Spillway of the Jingping-1Hydropower Station (in Chinese)